Science of the Total Environment 954 (2024) 176335

Contents lists available at ScienceDirect

Science of the Total Environment

journal homepage: www.elsevier.com/locate/scitotenv

Evaluation of the phytotoxicity and accumulation potential of nitro-polycyclic aromatic hydrocarbon, 3-nitrofluoranthene, on water status, photosystem II efficiency, antioxidant activity and ROS accumulation in *Salvinia natans*

Fatma Nur Alp-Turgut [a], Evren Yildiztugay [a,*], Ceyda Ozfidan-Konakci [b,*], İsmail Tarhan [c], Melek Öner [c], Cagri Gulenturk [a]

[a] Department of Biotechnology, Faculty of Science, Selcuk University, 42130, Konya, Turkey
[b] Department of Molecular Biology and Genetics, Faculty of Science, Necmettin Erbakan University, 42090, Konya, Turkey
[c] Department of Biochemistry, Faculty of Science, Selcuk University, 42130, Konya, Turkey

HIGHLIGHTS

- 3-NF toxicity reduced growth and carbon assimilation in *S. natans*.
- Phenomenological energy fluxes were altered by 3-NF treatments.
- *S. natans* couldn't maintened photosynthetic efficiency.
- Antioxidant enzymes were effective in tolerance to <250 μM 3-NF.
- *S. natans* has the potential to be used in the phytoremediation of 3-NF pollution.

GRAPHICAL ABSTRACT

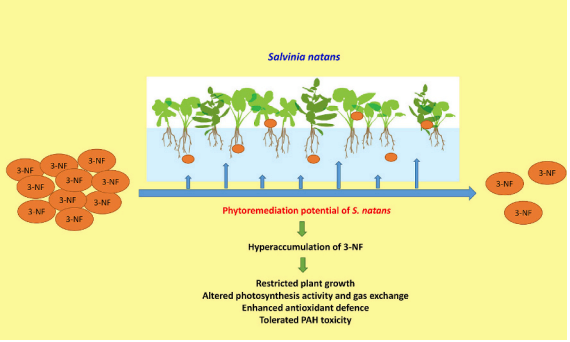

ARTICLE INFO

Editor: Henner Hollert

Keywords:
Antioxidant system
PAH toxicity
Phytoremediation
Salvinia natans
3-nitroflouranthene

ABSTRACT

Organic pollutants, which have become one of the most striking problems of today, raise concerns about the spread of polyaromatic hydrocarbon (PAH) compounds into ecosystems and their toxic effects on living organisms. The purpose of this study was to determine how harmful 3-nitrofluoranthene (3-NF) exposure was to *Salvinia natans*, a freshwater macrophyte. Furthermore, it clarifies how this aquatic plant, which is frequently used in phytoremediation of water contaminants and wastewater treatments, interacts with PAHs and contributes to the development of bioremediation methods. In *S. natans* exposed to stress (10 μM (3-NF10), 25 μM (3-NF25), 50 μM (3-NF50), 100 μM (3-NF100), 250 μM (3-NF250), 500 μM (3-NF500), 1000 μM (3-NF1000) 3-nitrofluoranthene), 3-NF accumulation, oxidative stress indicators, photosynthetic efficiency, and antioxidant system activity alterations were investigated for this objective. The findings demonstrated that *S. natans* could effectively accumulate 3-NF, and at a concentration of 1000 μM, the 3-NF content in the leaves reached approximately 1112 mg/kg. While its adverse effects on growth (RGR) and photosynthesis (F_v/F_m) remained

* Corresponding authors.
E-mail addresses: fatmanur.alp@selcuk.edu.tr (F.N. Alp-Turgut), eytugay@selcuk.edu.tr (E. Yildiztugay), cozfidan@erbakan.edu.tr (C. Ozfidan-Konakci).

https://doi.org/10.1016/j.scitotenv.2024.176335
Received 27 May 2024; Received in revised form 11 August 2024; Accepted 15 September 2024
Available online 17 September 2024

mild up to a concentration of 250 μM, the severity of the inhibitions increased at higher concentrations. On the other hand, exposure to 3-NF triggered the antioxidant system in *S. natans* plants and resulted in an increase of 60 %, 80 %, 47 % and 27 % in superoxide dismutase (SOD) activity in 3-NF10–25–50-100 groups, respectively. Conversely, in comparison to control plants, higher concentrations of 3-NF treatments resulted in insufficient antioxidant activity, increased lipid peroxidation (TBARS concentration), and hydrogen peroxide (H_2O_2). In conclusion, *S. natans* plants tolerated 3-NF accumulation up to 250 μM concentration despite limitations in growth suppression and photosynthetic capacity, proving that *S. natans* has the potential to be used in phytoextraction studies of 3-NF-polluted waters.

1. Introduction

In the past few years, there has been a surge in industrial, agricultural, and technological breakthroughs due to the pressing needs of social progress and the world population growth. The natural environment is under a tremendous deal of strain due to the rising use of natural resources, energy consumption, and waste generation to meet human demands. This has resulted in environmental deterioration and changes in the composition of many environmental media, including water (Sokol et al., 2022). Furthermore, a large number of new organic compounds are introduced to the global market each year; these compounds, which include pharmaceuticals, pesticides, personal care items, and surfactants that contain polycyclic aromatic hydrocarbons (PAHs), are used extensively in industrial activities across the globe. These substances, which then become permanent by being discharged into various water bodies, create major health and environmental issues (Barbosa Jr et al., 2023). As a result of the growth of anthropological activities, water pollution and a lack of access to clean water have consequently become widespread issues (Akinpelumi et al., 2023).

Organic substances like PAHs have been frequently detected in aquatic habitats lately. According to recent studies, PAHs can be found in a variety of aquatic ecosystems, including saltwater, groundwater, surface water, influent and effluent from wastewater treatment areas, and groundwater (Adeola and Forbes, 2021). PAHs are generated by both natural and human-caused activities related to urbanization and industrialization. It is thought that pyrogenic sources like volcanoes and the combustion of plant and petroleum compounds are the source of the majority of PAHs. 400 PAH species and their cytotoxic consequences have been identified, which are very difficult to biodegrade due to their hydrophobic and lipophilic nature (Barbosa Jr et al., 2023; Bright et al., 2023). By interfering with a number of physiological functions, including photosynthesis, respiration, and nutrient intake, PAHs may directly damage plants (Jia et al., 2023). PAHs can also alter a number of parameters significantly, such as growth, water retention capacity, and chlorophyll gas exchange (Akash et al., 2022). For example, *Cucumis sativus* subjected to phenanthrene toxicity demonstrated suppression of fresh weight and photosynthesis, according to Guo et al. (2021). Similarly, an earlier study indicated that anthracene induces modifications in the total content of photosynthetic pigments and a reduction in plant biomass in *Marchantia polymorpha* (Spinedi et al., 2021). Additionally, photosynthetic indices such as net photosynthetic rate (P_n), stomatal conductance (g_s), and intercellular CO_2 concentration (C_i) reduced in *Alternanthera philoxeroides* as the phenanthrene or pyrene concentrations increased (Huang et al., 2018). Oxidative stress, which can disrupt plant cell membranes, proteins, and DNA, is the cause of all these alterations (He et al., 2023). Based on previous studies, PAHs can trigger an increase in reactive oxygen species (ROS), which could result in oxidative stress. Within *A. thaliana* was exposed to PAHs, which resulted in a marked increase in ROS generation, concurrent plant tissue necrosis, and consequent growth suppression (Molina and Segura, 2021).

All things considered, the harmful effects of PAHs on plants can lead to serious ecological and economic implications, including reduced crop yields and reduced biodiversity. Therefore, in order to protect plants and the ecological balance, it is essential to prevent or minimize the release of PAHs into the environment, primarily through aquatic systems (Song et al., 2022). The majority of the technologies developed to date for this goal are costly or have the potential to cause harm to ecosystems, among other issues. However, pollutants can be immobilized, inactivated, decomposed, or removed from the environment by plants using a technique described as phytoremediation, which is efficient, low-cost, sustainable, and ecologically friendly (Sharma et al., 2023). Hyperaccumulator plants are 100 times more capable than non-accumulator plants at removing organic pollutants from the environment and accumulating them by phytoextraction. On the other hand, certain physiological and biochemical alterations may result from the buildup of contaminants in plants (Singh et al., 2023). Consequently, in the process of phytoremediation of PAHs, some plant species are more suited for utilizing the phytoextraction method. Regarding water pollution, a number of macrophytes have been investigated for their capacity to absorb, accumulate, and degrade various aspects of pollutants in both natural and artificial wetlands and it has been observed that these macrophytes can balance the concentration of organic pollutants, heavy metals, and nutrients in wetlands (Ekperusi et al., 2020; Saha et al., 2022).

The existence of hyperaccumulator plants is an essential component of the phytoremediation process. Previous studies on the removal, uptake, and accumulation of PAHs by plants have focused mainly on terrestrial plants and a few species of wetland, for example, *Medicago sativa* and *Phragmites australis*. Another study also showed the accumulation and translocation of PAHs in *O. sativa*. Also, *Helianthus annuus* was also proven to have a great potential to accumulate PAHs (Rajput et al., 2021). However, *Salvinia natans* is one example of an aquatic macrophyte that has been found to be employed as a hyperaccumulator in phytoextraction. Although previously, the advantages of using *S. natans* in this process have been well documented (Biju et al., 2023; Sitarska et al., 2023; Srivastava, 2023), the physiological and biochemical responses under one of the most common pyrogenic PAH, which has little bioavailability due to low water solubility, 3-nitrofluoranthene (3-NF) stress and phytoremediation potential remain unclear. In this regard the present study aims to investigate the following specific objectives: (1) To assess the impact of 3-NF stress on the growth, photosynthetic efficiency, and antioxidant activity of *S. natans*; (2) To ain the potential for 3-NF accumulation by *S. natans*; and (3) To reveal the tolerance limit and detoxification mechanisms of *S. natans* against 3-NF stress through physiological and biochemical analysis. The acquired data offer crucial details on *S. natans*'s capacity for phytoremediation in the 3-NF-polluted environment.

2. Materials and methods

2.1. Experimental design and treatments

Salvinia natans plants were raised in hydroponic hoagland solution under controlled conditions (16/8 h light/dark regime at 24 °C, 70 % relative humidity, and 350 μmol m^{-2} s^{-1} photosynthetic photon flux density). For stress applications, 10 μM (3-NF10), 25 μM (3-NF25), 50 μM (3-NF50), 100 μM (3-NF100), 250 μM (3-NF250), 500 μM (3-NF500), 1000 μM (3-NF1000) 3-nitrofluoranthene (3-NF) were treated for 7 days. Eight groups made up the experiment, which is listed in Supplementary File S1. Following a one-week treatment period, plants

were collected and rinsed with deionized water.

2.2. Extraction of 3-nitrofluoranthene from the leaves and analysis by GC–MS

For the extraction of uptake 3-NF in plant leaves, the method proposed by Culotta et al. (2005) was applied with some modifications. 2.00 g of fresh leaf sample was weighed for the extraction. Weighed samples from both control and 3-NF-applied were homogenized by grinding with a mortar in liquid nitrogen, then transferred into volumetric flask of appropriate volume. The samples were treated with a 40 mL of dichloromethane in an ultrasonic bath at room temperature for 20 min. After the organic phase was separated, the same process was performed 2 more times on the rest. The supernatant was taken into a separate volumetric flask and concentrated to approximately 2 mL in a rotary evaporator at 35 °C around. The concentrated organic phase was gently treated with nitrogen gas to completely remove the solvent and the remaining dissolved in 1.5 mL of dichloromethane. After taking 200 μL of this solution and dissolving it with 1 mL dichloromethane, it was passed through a syringe filter containing a polytetrafluoroethylene (PTFE) membrane with a pore size of 0.45 μm and placed in a capped glass vial with a volume of 1.5 mL, making it ready for chromatographic analysis. Standard 3-NF was obtained and diluted with dichloromethane at different rates to create calibration solutions to be used in the chromatographic analyzes to determine the 3-NF uptake in the leaf samples.

An Agilent (CA, USA) 7890 N-5975C GC system with a Chemstation data processor (Ver. B.03.02) was used to analyze the 3-NF concentration in the samples. The column was an Agilent (CA, USA) HP-5MS capillary column (30 m × 0.25 mm × 0.25 μm, (5 %-phenyl)-methylpolysiloxane). The temperature program of the column oven was as follows: at 50 °C for 2 min, then increased at 10 °C/min from 50 °C to 200 °C, held at 200 °C for 10 min, and increased at 20 °C/min from 200 °C to 280 °C, held at 280 °C for 2 min. The carrier gas was helium; the flow rate was 0.7 mL/min; the temperature of the injection block was 180 °C. The electron ionization mode of MS was 70 eV; the sample injection volume was 1.0 μl on splitless mode. The temperatures of the quadrupole and source in the MS block were 150 °C and 230 °C, respectively. The full MS scan mode was performed.

2.3. Growth and water content

The relative growth rate (RGR) was determined according to the procedure suggested by Hunt et al. (2002). Six plants were used for the control group and each treatment group. After the samples were oven-dried, dry weights were measured. RGR values were calculated according to the following formula:

$$RGR = \frac{[ln(DW_2) - ln(DW_1)]}{(t2 - t1)}$$

where t_1 and t_2 are initial and final harvest times, respectively DW1 is dry weight (g) at t_1; DW2 is dry weight (g) at t_2.

The relative water content (RWC) of leaves was calculated according to the method recommended by Smart and Bingham (1974). *S. natans* plants were harvested after 7 days and their fresh weight (FW) was evaluated. Before estimating turgid weight (TW), the leaves were floated in deionized water for 6 h. Following oven drying at 70 °C, the dry weight was obtained. The formula below was used to calculate the leaf's relative water content (RWC).

$$RWC\ (\%) = \frac{(FW - DW)}{(TW - DW)} \times 100$$

2.4. Photosystem II efficiency and OJIP analysis

Hansatech Instruments Ltd.'s Handy PEA (Plant Efficiency Analyzer) was used to find alterations in the PSII's photochemistry. The descriptions for the estimated parameters are included in Supplementary File S2. The average parameter values of treatment groups in *Salvinia natans* plants are represented in the radar plots.

2.5. Gas exchange parameters

A portable gas exchange device (LCpro+; ADC, Hoddesdon, UK) was used to test the gas exchange parameters of *Salvinia natans* leaves (Zhang et al., 2019).

2.6. Determination of H_2O_2 content, and lipid peroxidation

Hydrogen peroxide (H_2O_2) content of the leaf samples was identified as Liu et al. (2010) reported. The leaves were centrifuged after being homogenized in cold acetone. The titanium-peroxide complex was precipitated by adding ammonium hydroxide after the supernatant and titanium reagent had been combined. The mixture for the reaction was centrifuged. The pellet was dissolved after being rinsed with cold acetone. At 410 nm, the solution's absorbance was quantified. Using a standard curve created with known H_2O_2 values, H_2O_2 concentrations were computed. Lipid peroxidation level (measured as the concentration of thiobarbituric acid reactive compounds, or TBARS) was assessed in accordance with Rao and Sresty (2000). The absorbance at 532 nm was used to compute the concentration of TBARS, and results were adjusted for nonspecific turbidity by deducting the absorbance at 600 nm. A 155 mM^{-1} cm^{-1} extinction coefficient was used to determine the levels of TBARS.

2.7. Determination of enzymatic/non-enzymatic antioxidants

0.5 g leaf samples were extracted in Tris-HCl (25 mM Tris, 1 % Triton-X100, pH: 7.4) and centrifuged at 14000 *g* for 30 min. Supernatants were collected, and total protein contents were measured by the Bradford (1976) method.

For SOD (EC 1.15.1.1) isozyme activity, samples were subjected to non-denaturing polyacrylamide gel electrophoresis (PAGE) as described by Laemmli (1970). Total SOD activity assay was based on the method of Beauchamp and Fridovich (1971). CAT isozymes were detected according to Woodbury et al. (1971). Total CAT (EC 1.11.1.6) activity was estimated according to the method of Bergmeyer (1970). The isozymes and enzyme activity of POX (EC 1.11.1.7) were based on the method described by Seevers et al. (1971) and Herzog and Fahimi (1973), respectively. NADPH oxidase (NOX) isozymes were identified as described by Sagi and Fluhr (2001). NOX (EC 1.6.3.1) activity was measured according to Jiang and Zhang (2002). The enzyme/isozyme activities of glutathione S-transferase (GST, EC 2.5.1.18) and glutathione peroxidase (GPX, EC 1.11.1.9) were determined (Hossain et al., 2006; Ricci et al., 1984).

Electrophoretic APX separation was performed according to Mittler and Zilinskas (1993). APX (EC 1.11.1.11) enzyme activity was measured according to Nakano and Asada (1981). GR (EC 1.6.4.2) activity was measured according to Foyer and Halliwell (1976). Isozymes compositions of GR were determined by native PAGE analysis (Hou et al., 2004).

Monodehydroascorbate reductase (MDHAR; EC 1.6.5.4) activity was assayed by the method of Miyake and Asada (1992). Dehydroascorbate reductase (DHAR; EC 1.8.5.1) activity was measured according to Dalton et al. (1986). Total and reduced ascorbate (AsA) contents were done according to the method of Dutilleul et al. (2003) with modifications. The oxidized form of ascorbate (DHA, dehydroascorbate) was measured using the formula DHA = Total AsA-Reduced AsA. The glutathione (GSH) was assayed according to Paradiso et al. (2008). Oxidized glutathione (GSSG) was determined after the removal of GSH by 2-vinylpyridine derivatization. GSH redox state (%) was determined by calculating the ratio of GSH to total glutathione (GSH + GSSG) according to Shi et al. (2013).

Gels stained for SOD, CAT, POX, APX, GR, GST, and NOX activities

were photographed with the Gel Doc XR+ System and then analyzed with Image Lab software v4.0.1 (Bio-Rad, California, USA). Known standard amounts of enzymes (0.5 units of SOD and 0.2 units of CAT and POX) were loaded onto gels. For each isozyme set/group, the average values were significantly different at $p < 0.05$ using Tukey's post-test.

2.8. Statistical analysis

Six biological replicates and technical triplicates of each set of data were provided. All studies made use of one-way analysis of variance (ANOVA). The values were statistically analyzed using SPSS 23.0. Differences were deemed significant at $p < 0.05$.

3. Results

3.1. Effects of 3-nitrofluorantene on growth (RGR) and water content (RWC) in Salvinia natans and GC–MS chromatogram

Applications of 3-NF to *Salvinia natans* led to a consistent reduction in RGR values with increasing dose, as Fig. 1A illustrates. While the decrease in growth occurred less in low doses of treatments, it reduced rapidly especially after 250 μM. After 3-NF1000 was applied, the reductions in RGRs relative to the control reached a maximum and were recorded at 79.5 %. Investigation of the RWC levels revealed results at the control level up to the 3-NF50 group (Fig. 1B). However, these protected RWC values began to diminish in the 3-NF100 group and kept declining as the concentration increased when compared to control plants. The GC–MS chromatogram of the plant sample to which 1000 μM 3-NF was applied is given in Fig. 1C. As can be seen from the relevant Fig., the retention time of 3-nitro-fluoranthene is 43 min. The chromatograms of other 3-NF applied-plant samples are given in Supplementary File S3. 3-NF contents determined as a result of 3 replicate GC–MS analysis of the leaf samples in which 3-NF was applied at different concentrations are given in Table 1. Since PAH derivatives can be found in working environments as a result of plastic pollution, a blank test was conducted without leaf sample. In Table 1, the result of 0.00 obtained from the blank test shows that the equipment and analysis environment used are not exposed to pollution in terms of 3-NF. Considering the amount of 3-NF accumulated, *S. natans* showed a content increase proportional to the application concentration, especially after 50 μM 3-NF treatment.

3.2. Effects of 3-nitrofluorantene on gas exchange parameters in Salvinia natans

Considering the carbon assimilation rate (A) values of *Salvinia natans*, an approximately equal and average decrease of 25 % was detected in all groups up to the 3-NF100 group, compared to the control

Table 1
3-nitro-fluoranthene (3-NF) uptake of the leaf samples as a result of GC–MS analysis. The different letters are significantly different ($p < 0.05$) values.

3-NF (μM)	3-nitro-fluoranthene uptake (mg/kg leaf)
Blank	0.00 ± 0.00
Control	0.00^{a} ± 0.00
10	26.99^{b} ± 1.41
25	30.18^{c} ± 2.16
50	25.54^{b} ± 2.98
100	46.36^{c} ± 3.57
250	161.88^{d} ± 1.22
500	439.09^{e} ± 17.26
1000	1112.89^{f} ± 5.26

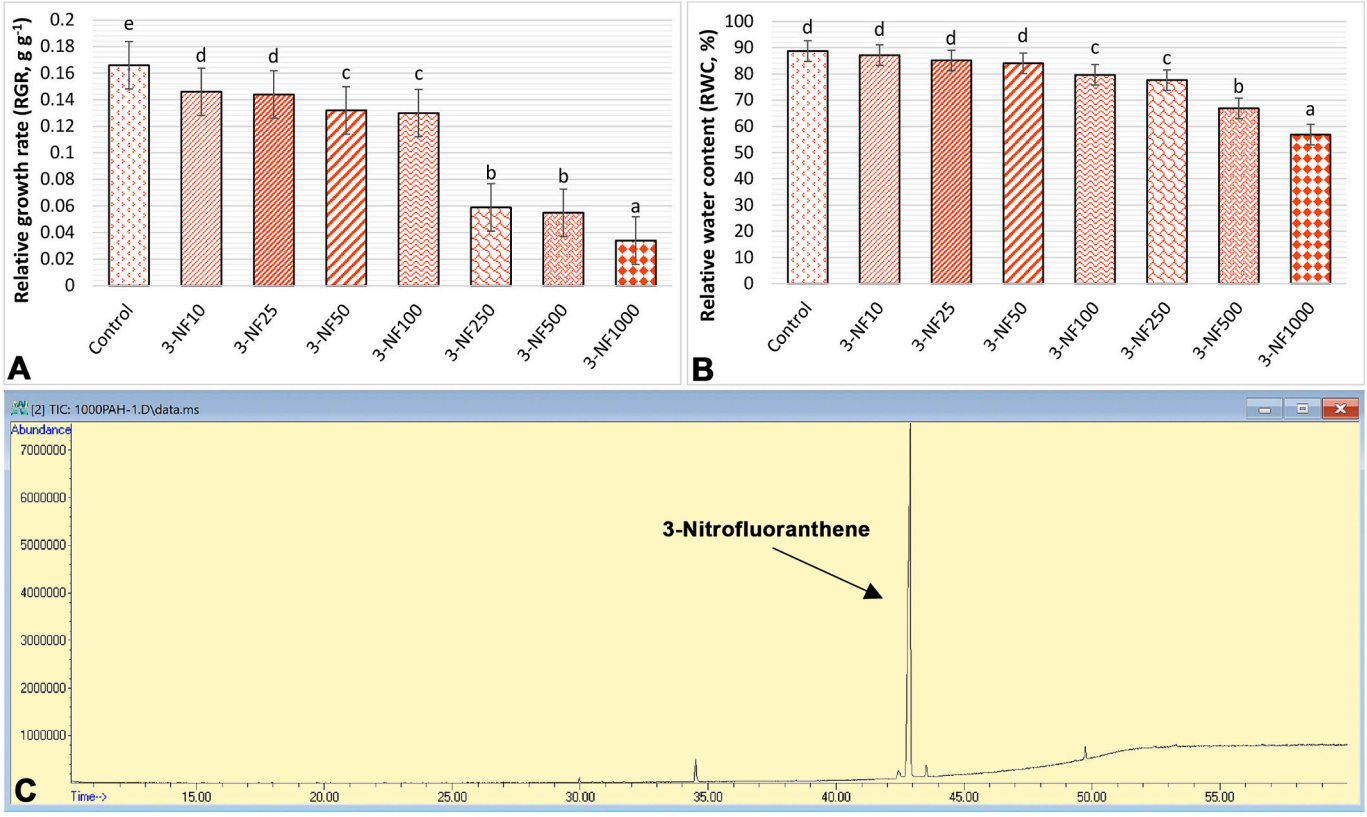

Fig. 1. The effects of 3-nitroflouranthene treatments (10 μM (3-NF10), 25 μM (3-NF25), 50 μM (3-NF50), 100 μM (3-NF100), 250 μM (3-NF250), 500 μM (3-NF500), 1000 μM (3-NF1000)) on the relative growth rate (RGR, %, A), the relative water content (RWC, %, B), and the GC–MS chromatogram of the 1000 μM 3-NF treated leaf (C) in *Salvinia natans*.

group (Fig. 2A). Starting from the 3-NF250 group, the inhibition level in A continued to increase. Stomatal conductance (g_s) levels were similar to control levels up to a concentration of 500 μM 3-nitrofluoranthene (3-NF), as shown in Fig. 2B. These values increased by 18.5 % in the 3-NF500 group and 66.5 % in the 3-NF1000 group with increasing concentrations. In 10–25-50 μM stress treatments, the intercellular CO_2 concentration (C_i) increased by around 2.3 % relative to the control (Fig. 2C). Following the 3-NF100 group, these values increased much further. The 3-NF250 group had the highest increase in C_i levels, measuring 10.6 %. Transpiration rates (E) of *Salvinia natans* did not significantly differ from the control until the 3-NF250 group (Fig. 2D). Nonetheless, increments in E were noted beginning with the 3-NF250 group. In comparison to the control, 3-NF treatments reduced stomatal limitation (L_s), as Fig. 2E indicates. These declines started to increase especially in the 3-NF100 group and peaked (72.8 %) in 3-NF1000 plants. In every stress group, the ratio of carboxylation efficiency (A/C_i) reduced (Fig. 2F). A/C_i results showed the highest declines, particularly at 250–500–1000 μM 3-NF doses.

3.3. Effects of 3-nitrofluorantene on photosynthetic yield in Salvinia natans

When comparing the F_v/F_m (maximal (or potential) quantum yield of PSII) levels of the 3-NF10–25–50-100-1000 groups to the control, there was a similar and average 5 % decrease (Fig. 3A). A higher decrease was observed at 250 (%7.7) and 500 μM (%6.5) concentrations. Similarly, *Salvinia natans*' F_v/F_o (potential photochemical activity of PSII) values decreased in response to all 3-NF concentrations (Fig. 3B). These decreases reached the highest level, especially in the 3-NF500 and 3-NF1000 groups with %28 and %23, respectively. As seen in Fig. 3C, F_o/F_m (physiological state of PSII) values of *Salvinia natans* tend to increase in all groups compared to the control. The highest increase was measured in the 3-NF500 and 3-NF1000 groups (approximately 62 % in both doses).

3.4. Effects of 3-nitrofluorantene on photosynthetic machinery in Salvinia natans

Fig. 4A displays the radar graph with the JIP test parameters computed from the treatment groups. 3-NF treatments reduced the

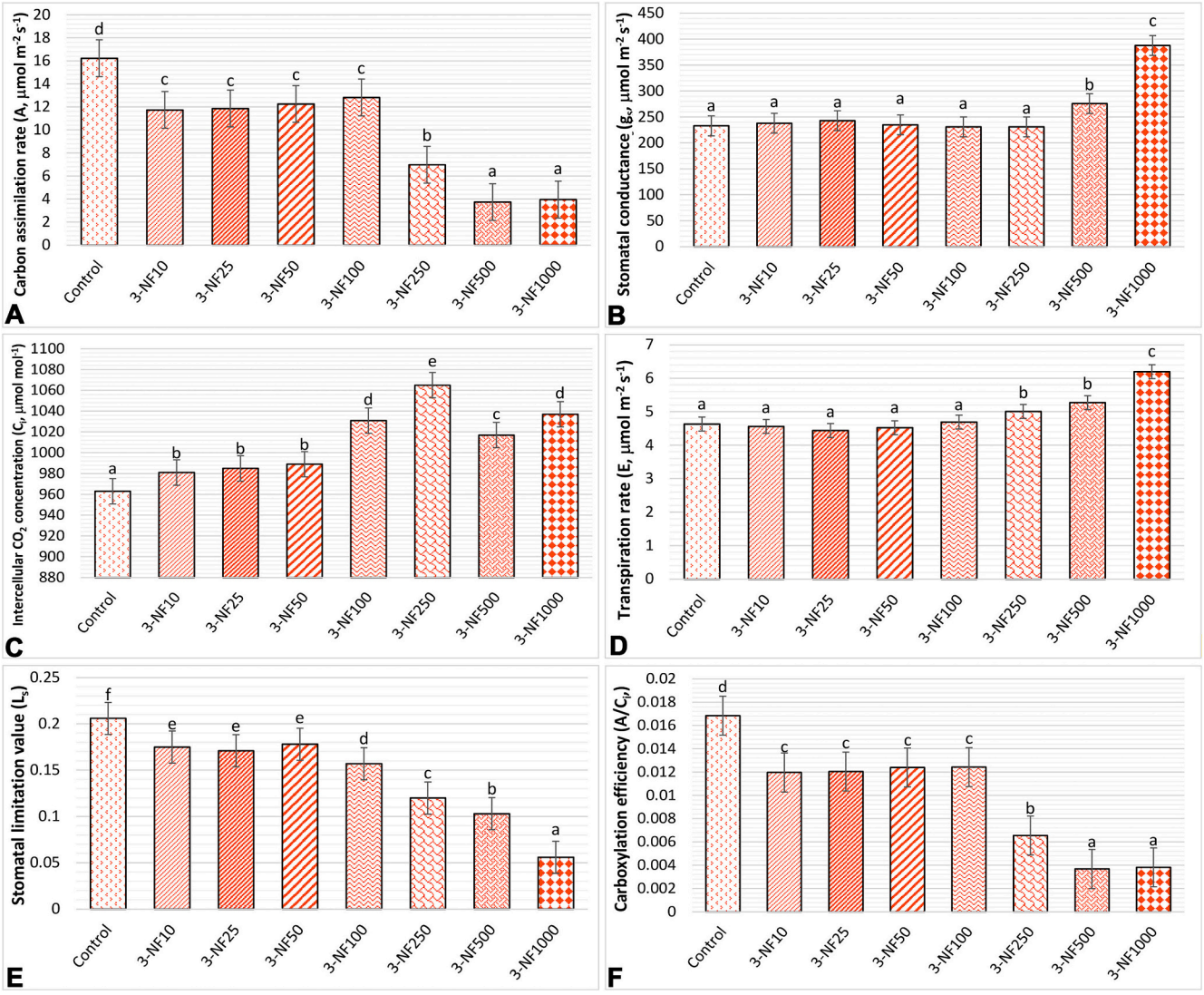

Fig. 2. The effects of 3-nitroflouranthene treatments (10 μM (3-NF10), 25 μM (3-NF25), 50 μM (3-NF50), 100 μM (3-NF100), 250 μM (3-NF250), 500 μM (3-NF500), 1000 μM (3-NF1000)) on the carbon assimilation rate (A, A), the stomatal conductance (g_s, B), the intercellular CO_2 concentrations (C_i, C), the transpiration rate (E, D), the stomatal limitation value (L_s, E), and the carboxylation efficiency (A/C_i, F) in *Salvinia natans*.

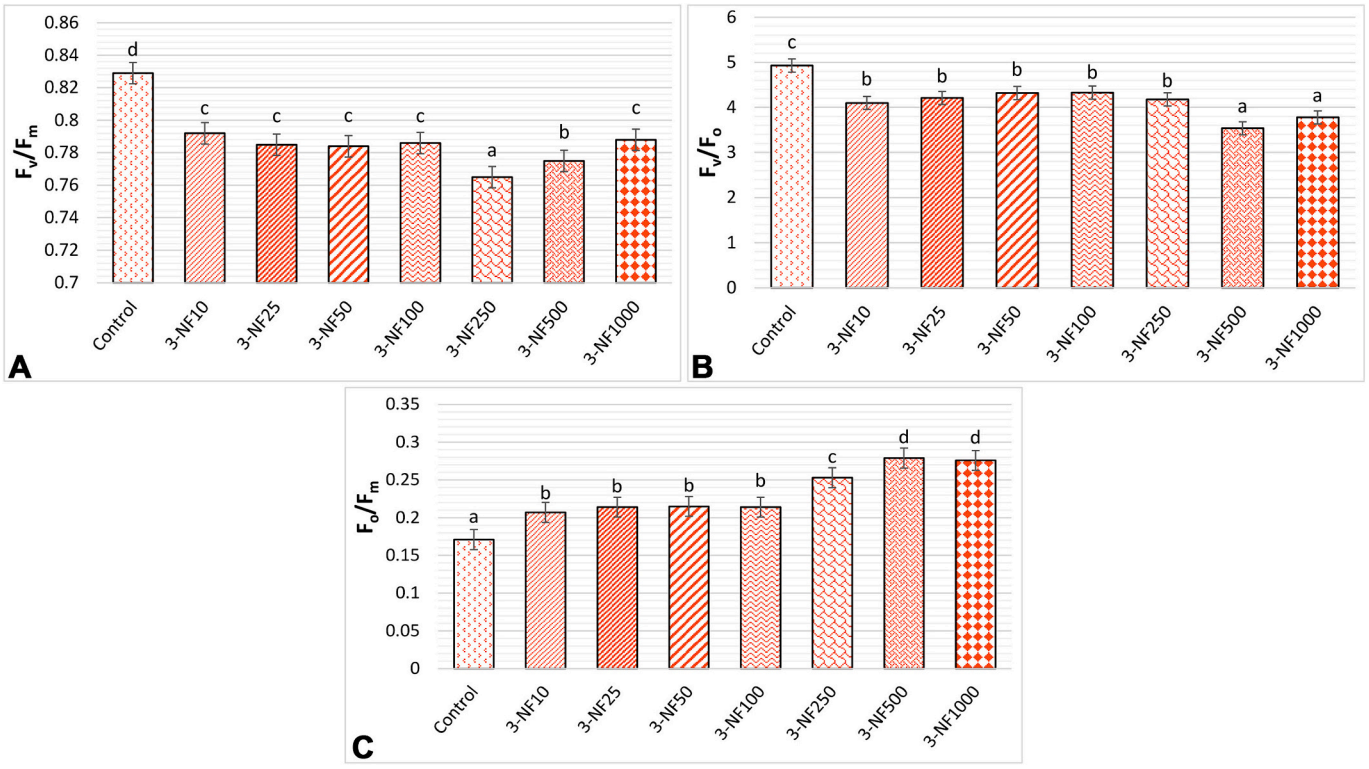

Fig. 3. The effects of 3-nitroflouranthene treatments (10 μM (3-NF10), 25 μM (3-NF25), 50 μM (3-NF50), 100 μM (3-NF100), 250 μM (3-NF250), 500 μM (3-NF500), 1000 μM (3-NF1000)) on the PSII photochemistry's maximum quantum yield (Fv/Fm, A), the predicted photochemical efficiency (Fv/Fo, B), and the physiological condition of the photosynthetic apparatus (Fo/Fm, C) in *Salvinia natans*.

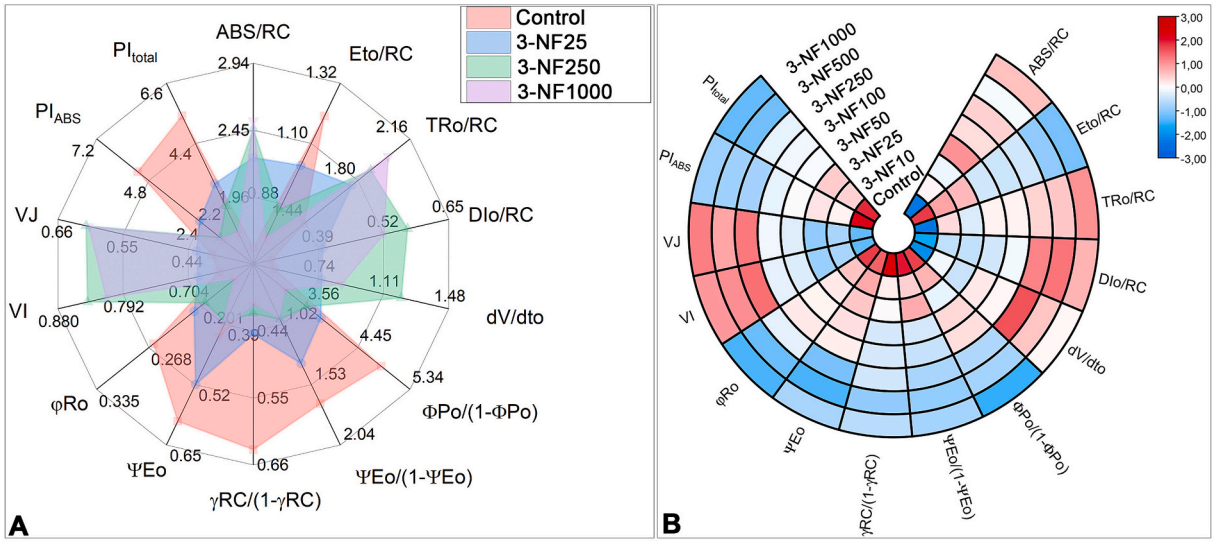

Fig. 4. The effects of 3-nitroflouranthene treatments (10 μM (3-NF10), 25 μM (3-NF25), 50 μM (3-NF50), 100 μM (3-NF100), 250 μM (3-NF250), 500 μM (3-NF500), 1000 μM (3-NF1000)) on the average absorption per active reaction centers (ABS/RC), electron transport flux per active reaction centers (ET_o/RC), flux or exciton trapped per active reaction center (TR_o/RC), Q_A-reducing RCs per photosystem II antenna chlorophyll ($\Phi P_o/(1-\Phi P_o)$), the efficiency of the trapped exciton to transfer an electron to the photosynthetic electron transfer chain ($\Psi E_o/(1-\Psi E_o)$), $Q_{\bar{A}}$ reducing reaction centers per photosystem II antenna chlorophyll ($\gamma RC/(1-\gamma RC)$), ratio of total dissipation to the amount of active reaction center (DI_o/RC), performance index based on the absorption of light energy (PI_{ABS}) and performance index for energy savings from excitons to the reduction of photosystem I and acceptors (PI_{total}) in *Salvinia natans*.

values of ET_o/RC (electron transport per reaction center: beyond $Q_{\bar{A}}$), $\Psi E_o/(1-\Psi E_o)$ (the efficiency with which a trapped exciton transfers an electron to the photosynthetic electron transfer chain), $\Phi P_o/(1-\Phi P_o)$ (Q_A-reducing reaction centers per PSII antenna chlorophyll), $\gamma RC/(1-\gamma RC)$ (the efficiency with which a trapped exciton transfers an electron to the photosynthetic electron transfer chain), performance index in the way of energy absorption (PI_{ABS} and PItotal) in *S. natans*. On the other hand, all stress doses increased the energy loss (DI_o/RC), specific energy flows from the reaction centers (ABS/RC), and energy trapping per reaction center (TRo/RC) compared to control. Fig. 4B showed the levels of fluorescence-related parameters by color scale. Here, colors ranging from blue to red indicate low to high induction.

3.5. Effects of 3-nitrofluoranthene on hydrogen peroxide (H_2O_2) content and lipid peroxidation in Salvinia natans

3-NF applications did not cause a significant change in the H_2O_2 contents of *Salvinia natans* at 10–25–50-100 μM concentrations compared to the control (Fig. 5A). Conversely, increases were triggered after 250 μM treatment. With an increase of 35 % over the control, the 3-NF1000 group had the highest content. Similarly, lipid peroxidation levels (TBARS content) in all groups up to 100 μM concentration were similar to control plants (Fig. 5B). However, this stagnation in TBARS contents was disrupted at higher doses.

3.6. Effects of 3-nitrofluorantene on antioxidant system-related enzyme and isoenzyme activities in Salvinia natans

Fig. 6A shows the presence of seven superoxide dismutase isozymes in the isozyme assay of *Salvinia natans*, including Mn-SOD1–2–3-4-5 and Fe-SOD1–2. According to the band intensities of all isozymes, *S. natans* that were exposed to 3-NF treatments exhibited elevated SOD activity at all concentrations from the 3-NF10 to the 3-NF100 group in comparison with the control (Fig. 6B). However, at concentrations of 250–500-1000 μM, SOD activities were similar to control plants. Four catalase isozymes (CAT1–2–3-4) were revealed in *S. natans* (Fig. 6C). As seen in Fig. 6D, CAT activities were higher in the 3-NF10–50-100 groups compared to the control. On the other hand, no significant alteration was detected in the 3-NF25 group. CAT activity reduction was induced by higher 3-NF concentrations.

Fig. 7A illustrates that ten bands (POX1–10) were identified for POX isoenzymes in *S. natans*. When the results of 3-NF applications were examined, consistent increases were detected depending on the dose, compared to the control, up to the 3-NF100 group (Fig. 7B). Contrary to these results, at higher stress concentrations POX activities were lower compared to the control. These changes in POX activities were correlated with all POX isozyme band intensities (Fig. 7A). *S. natans* contains ten GST isoenzymes (GST1–10), as seen in Fig. 7C. As shown in Fig. 7D, 3-NF treatments increased the GST activities up to the 3-NF100 group compared to the control. The highest increase, 2-fold, was measured in 3-NF100 group. These modifications resulted from band intensities in all GST isoforms (Fig. 7C). In contrast, there were decreases in GST activities of the 3-NF250–500 groups. At 1000 μM stress application, this activity was similar to the control level (Fig. 7D).

Three NOX isoforms (NOX1–3) were identified through analysis of NOX isoenzymes in *S. natans* (Fig. 8A). NOX activities increased significantly at approximately the same rate (82 %) up to a concentration of 100 μM after stress treatments (Fig. 8B). However, while approximately 24 % decreases in the NOX activities of *S. natans* were recorded in the 3-NF250 and 3-NF1000 groups, no significant change was observed in the 3-NF500 (Fig. 8B). These changes were parallel with all isozyme densities (Fig. 8A). Three GPX isoforms (GPX1–3) were detected in *S. natans* as seen in Fig. 8C. 10–25–50-100 μM treatment with 3-NF resulted in increases in GPX activity (Fig. 8D). In contrast, under 250 μM stress conditions, GPX activity tended to decrease. At higher concentrations, GPX activities were at control levels. All of these modifications in GPX activity were consistent with the band intensities of GPX1 and GPX2 in particular (Fig. 8C).

3.7. Effects of 3-nitrofluorantene on enzyme and non-enzyme activities/contents associated with the AsA-GSH cycle in Salvinia natans

In this study, three APX isoforms (APX1–3) were found throughout the experiment (Fig. 9A). 3-NF stress treatments induced APX activity in 3-NF10–25–50-100 groups (Fig. 9B). These increases were especially notable in the 3-NF10 and 3-NF25 groups. However, when higher 3-NF stress than 100 μM was given, significant decreases in APX activity were observed. In general, varying intensities of all bands had an impact on APX activities (Fig. 9A). Three isozymes (GR1–3) were found to evaluate GR isozymes, as shown in Fig. 9C. Similar to APX, 3-NF treatments up to 100 μM concentration increased GR activities compared to control (Fig. 9D). The highest increment belonged to 3-NF10 group plants, with approximately 87 %. On the other hand, 250 and 500 μM applications led to a decrease in GR activity. GR activities of the 3-NF1000 group were similar to the control. The band intensity of each isozyme provided evidence for these changes (Fig. 9C).

10–25-50 μM stress treatments caused increases in MDHAR activity compared to control plants, while 500 and 1000 μM concentrations resulted in decreases (Fig. 10A). On the other hand, the activity of MDHAR was not affected in the 3-NF100–250 groups. As demonstrated in Fig. 10B, 3-NF applications in *S. natans* increased the DHAR activities of the 3-NF10–25-50 groups. However, DHAR activity was found to be at a similar level to the control in the 3-NF100 group, while declines were observed in the 3-NF250–500-1000 groups. When compared to control groups, *S. natans* treated with 10–25-50 μM 3-NF had higher AsA contents (Fig. 10C). In contrast, stress at higher concentrations resulted in decreases in AsA contents. *S. natans* with 3-NF treatments exhibited reduced DHA contents up to the 3-NF100 group (Fig. 10D). However, 250–500-100 μM stress increased these values. The highest DHA level was detected in the 3-NF1000 group with approximately 2.13-fold. In line with the findings of AsA and DHA concentrations, AsA/DHA ratios were regulated in stressed *S. natans* (Fig. 10G). These rates increased in the 3-NF10–25-50 groups, were similar to the control level in the 3-NF100 group, but resulted in reductions at higher 3-NF doses. Compared to control plants, the highest increase in the AsA/DHA ratio was measured in the 3-NF10 group, with 3-fold. As shown in Fig. 10E, 10–25-50 μM stress treatments induced GSH contents. On the other hand, higher concentrations did not change or reduce GSH contents. The results presented in Fig. 10F revealed that, in contrast to GSH contents, 10–25-50 μM stress applications led to diminished GSSG levels. The GSSG level, which was not affected by the 100 μM concentration,

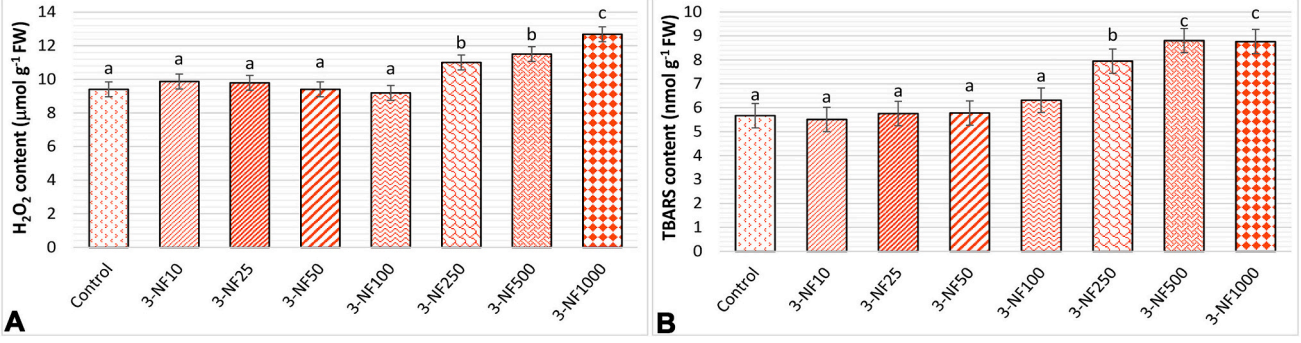

Fig. 5. The effects of 3-nitroflouranthene treatments (10 μM (3-NF10), 25 μM (3-NF25), 50 μM (3-NF50), 100 μM (3-NF100), 250 μM (3-NF250), 500 μM (3-NF500), 1000 μM (3-NF1000)) on the hydrogen peroxide content (H_2O_2, A) and the lipid peroxidation (TBARS, B) in *Salvinia natans*.

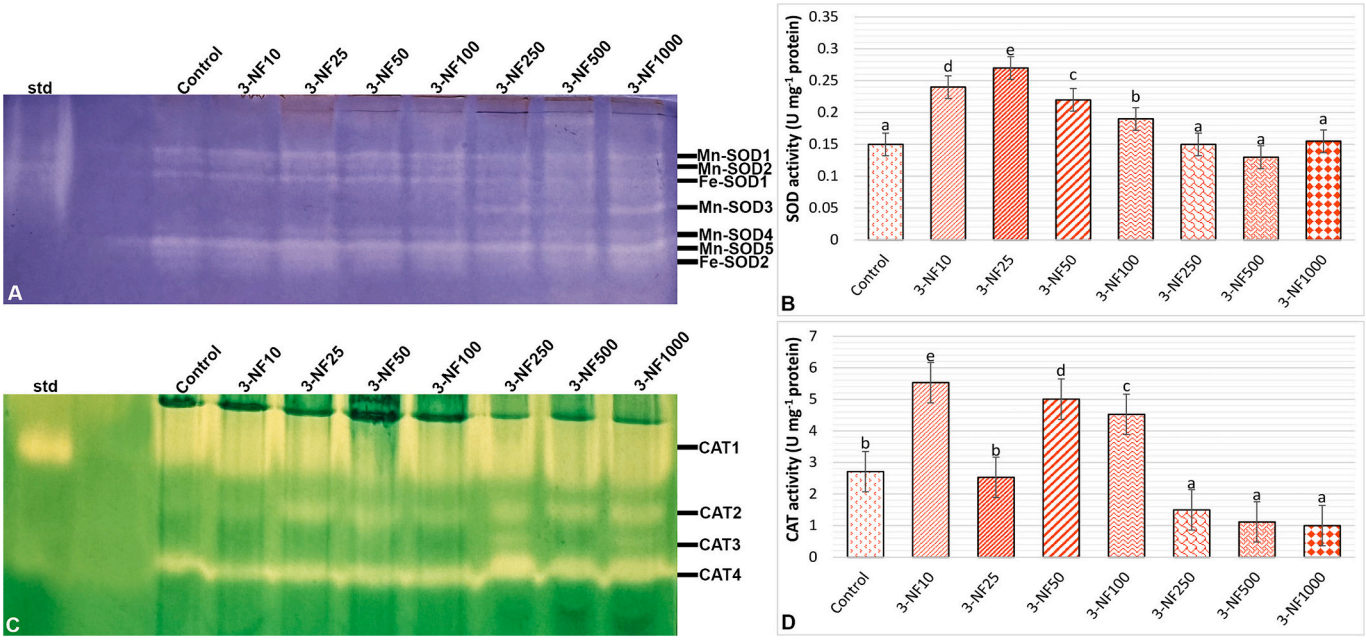

Fig. 6. The effects of 3-nitroflouranthene treatments (10 μM (3-NF10), 25 μM (3-NF25), 50 μM (3-NF50), 100 μM (3-NF100), 250 μM (3-NF250), 500 μM (3-NF500), 1000 μM (3-NF1000)) on the relative band strength of various types of superoxide dismutase isoenzymes (SOD, A) and SOD activity (B), the relative band strength of various types of catalase isoenzymes (CAT, C) and catalase activity (D) in *Salvinia natans*.

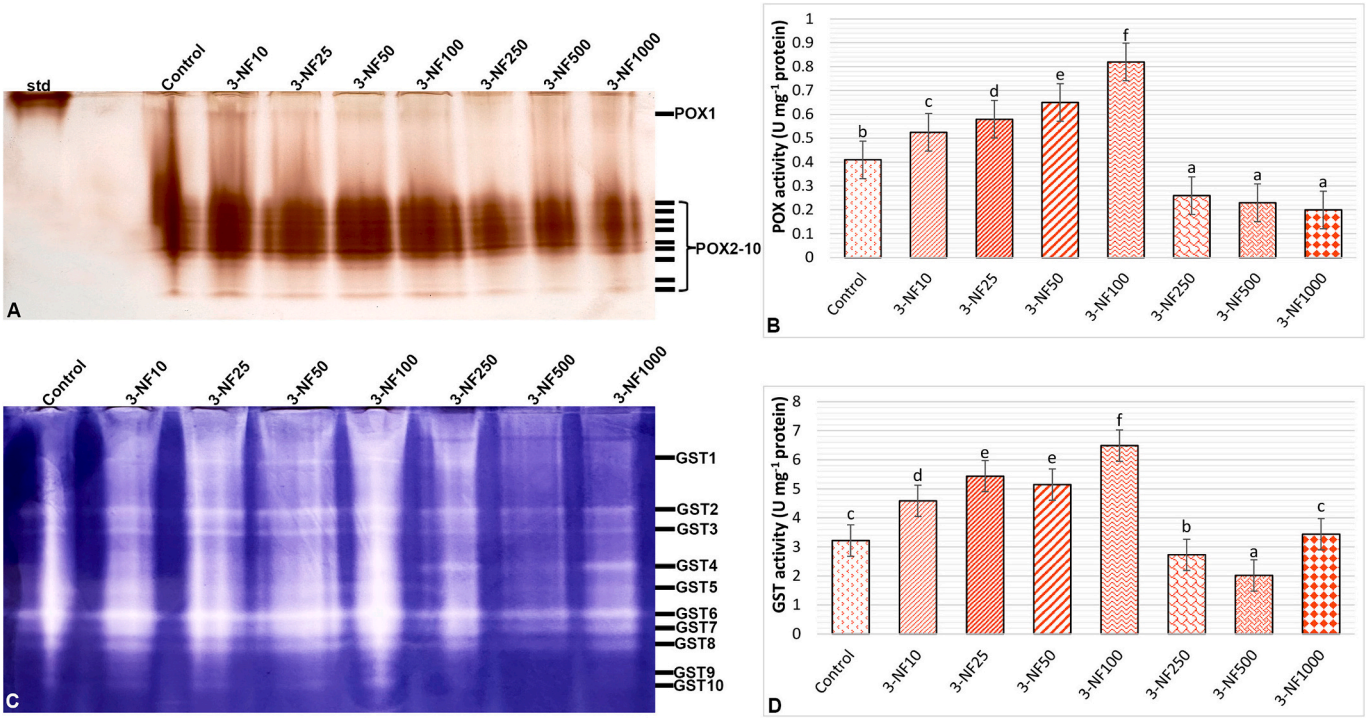

Fig. 7. The effects of 3-nitroflouranthene treatments (10 μM (3-NF10), 25 μM (3-NF25), 50 μM (3-NF50), 100 μM (3-NF100), 250 μM (3-NF250), 500 μM (3-NF500), 1000 μM (3-NF1000)) on the relative band strength of various types of peroxidase isoenzymes (POX, A) and POX activity (B), the relative band strength of various types of glutathione S-transferase isoenzymes (GST, C) and GST activity (D) in *Salvinia natans*.

exhibited increases compared to the control group at higher concentrations. Thus, levels in the GSH redox state also changed depending on these regulations (Fig. 10H).

4. Discussion

Water solubility, molecular weight, lipophilic property and structure of organic compounds such as PAHs determine their uptake and accumulation by plants (Zazouli et al., 2023). Accordingly, a GC–MS analysis was conducted to confirm the potential for 3-NF to enter and accumulate in *S. natans* leaves. Based on the findings, the plant's 3-NF concentration increased dramatically when the treatment doses were raised from 10 μM to 1000 μM. The results obtained demonstrated that *S. natans* efficiently accumulated 3-NF in leaves during the treatment period by

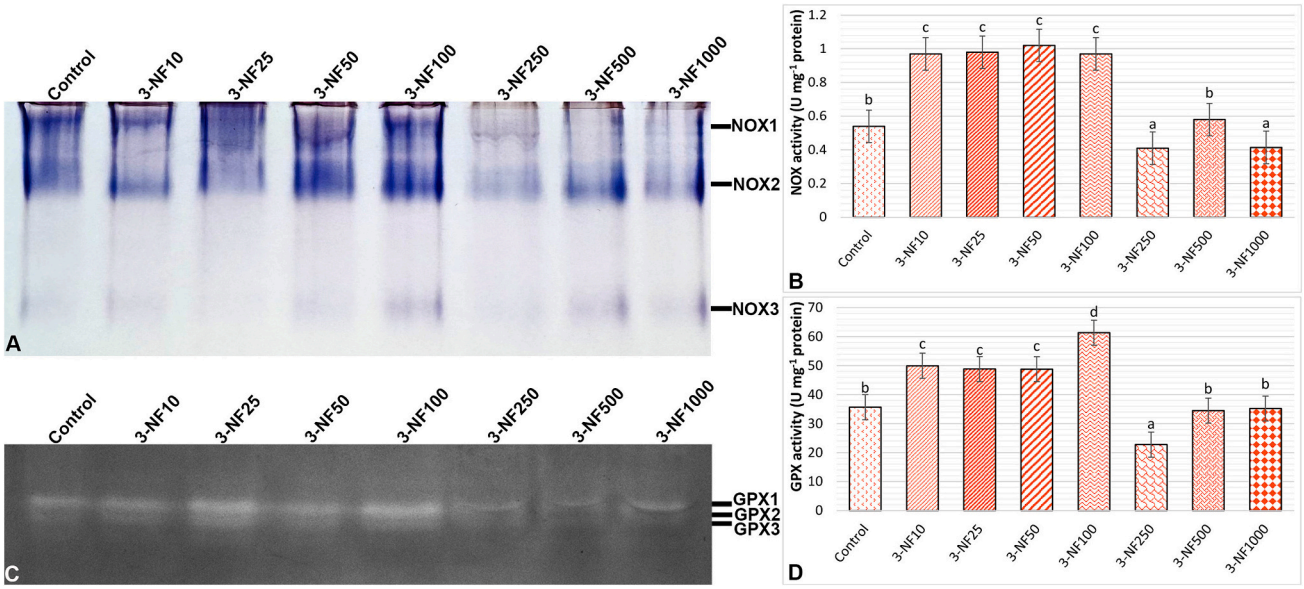

Fig. 8. The effects of 3-nitroflouranthene treatments (10 μM (3-NF10), 25 μM (3-NF25), 50 μM (3-NF50), 100 μM (3-NF100), 250 μM (3-NF250), 500 μM (3-NF500), 1000 μM (3-NF1000)) on the relative band strength of various types of NADPH-oxidase isoenzymes (NOX, A) and NOX activity (B), the relative band strength of various types of glutathione peroxidase isoenzymes (GPX, C) and GPX activity (D) in *Salvinia natans*.

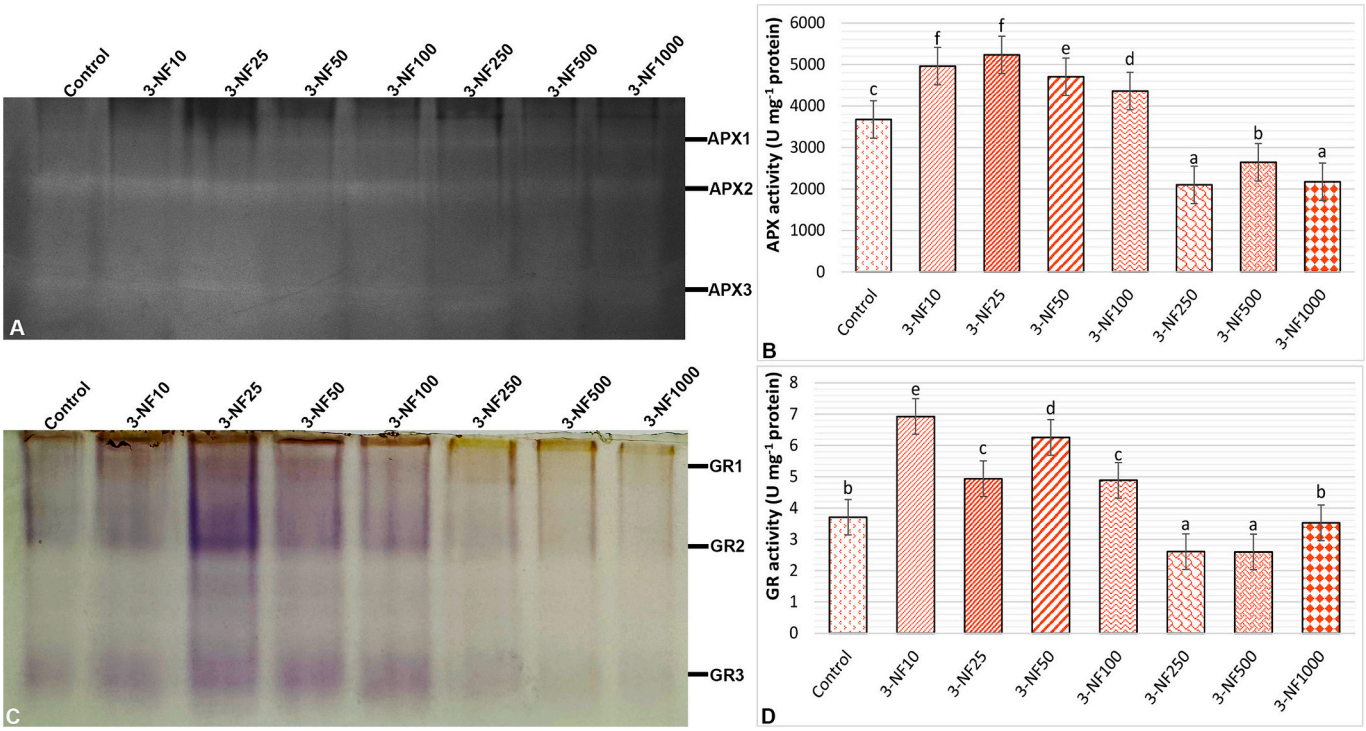

Fig. 9. The effects of 3-nitroflouranthene treatments (10 μM (3-NF10), 25 μM (3-NF25), 50 μM (3-NF50), 100 μM (3-NF100), 250 μM (3-NF250), 500 μM (3-NF500), 1000 μM (3-NF1000)) on the relative band strength of various types of ascorbate peroxidase (APX, A), and APX activity (B), the relative band strength of various types of glutathione reductase isoenzymes (GR, C) and GR activity (D) in *Salvinia natans*.

transferring it from the Hoagland solution to the leaves. PAHs with low molecular weight, such as 3-NF, are less stable than those with high molecular weight and can be more easily removed from the aquatic environment (Zhao et al., 2021). This is most likely the primary cause of *S. natans's* efficient absorption of 3-NF from Hoagland's medium. These observations are in line with the numerous recent studies of PAH bioaccumulation by a variety of plant species (Borah and Deka, 2024). Although the removal of 3-NF by *S. natans* leads to improved outcomes for the aquatic environment, accumulation of PAHs in plants can have various detrimental effects.

PAHs are toxic to plants and can adversely affect plant growth and development. On the other hand, the responses of plants to PAH compounds are related to various factors, such as the kind and amount of PAH, the length of exposure, and the type of plant (da Silva Correa et al., 2022). In the current study, a slight regression was observed in plant growth (RGR) starting from 10 μM 3-NF, but the severity of these

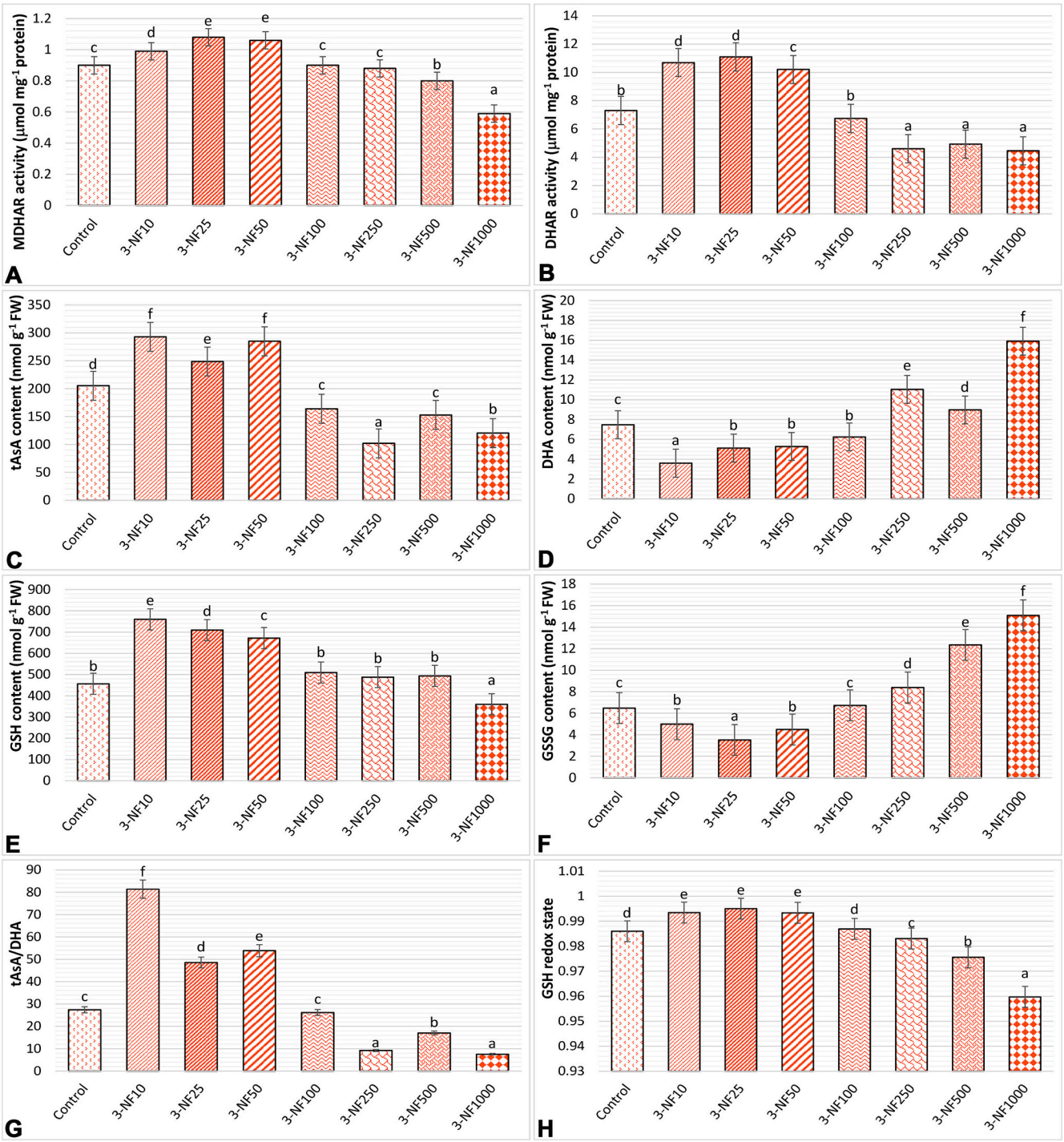

Fig. 10. The effects of 3-nitroflouranthene treatments (10 µM (3-NF10), 25 µM (3-NF25), 50 µM (3-NF50), 100 µM (3-NF100), 250 µM (3-NF250), 500 µM (3-NF500), 1000 µM (3-NF1000)) on the monodehydroascorbate reductase activity (MDHAR, A), the dehydroascorbate reductase activity (DHAR, B), the ascorbate content (tAsA, C), the dehydroascorbate content (DHA, D), the glutathione content (GSH, E), the oxidized glutathione content (GSSG, F), the AsA/DHA ratio (G) and GSH redox state (G) in *Salvinia natans*.

regressions increased especially from 250 µM concentration. In a similar study, triggered growth inhibition was observed in the *Axonopus compressus* plant, which is widely and successfully used in phytoremediation, exposed to PAH contamination (Hazaimeh et al., 2019). The possible reason for the decreases in growth is that PAHs cause growth inhibition in plants by directly interfering with several physiological functions involving photosynthesis, respiration and nutrient uptake (Jia et al., 2023). Moreover, leaf is the core organ in plants to be responsible for carbon fixation (i.e., photosynthesis) and is the central regulator for plant growth and development. Therefore, reductions in carbon assimilation of leaves, described in more detail below, may also be responsible for decreases in RGR (Hu et al., 2023). Also, PAHs cause reductions in water retention capacity in plants, that results in inhibition of photosynthetic activity and reduction in nutrient use efficiency (Sivaram et al., 2019). However, the results in this study showed that although RWC levels of *S. natans* plants decreased at high concentrations, they could be maintained without being affected by 3-NF concentrations of 100 µM and less. In this case, a possible reason for the growth inhibition

observed especially at high 3-NF concentrations may be this pattern in water content.

As with other abiotic stress conditions, chloroplasts are the first target of PAH stress attack. PAHs preferentially accumulate in the thylakoids of chloroplasts and microsomes, where they affect photochemical processes (Zhang et al., 2024a). It was pointed out in the current investigation that the effect of 3-NF on photosynthetic responses in *S. natans* was significantly related to its applied concentration. At concentrations below 250 μM, 3-NF slightly reduced the carbon assimilation rate (A). However, it significantly inhibited A when concentrations were above 250 μM. This outcome demonstrated that high 3-NF concentration and A in *S.natans* were negatively correlated. In the present research, A, and L_s decreased, but C_i increased, with 3-NF treatment, while g_s and E were generally at or higher than control levels. This demonstrated that non-stomatal limitation was the cause of the suppression of photosynthesis by 3-NF. The possible reason for this non-stomatal limitation may be that the accumulation of PAH compounds in chloroplasts may disrupt the thylakoid membranes of macrophytes, as reported by Sushkova et al. (2021). The light reaction and dark reaction phases of the photosynthetic carbon assimilation process must cooperate in order for photosynthetic efficiency to be achieved (Fu and Walker, 2023). To investigate the effect of 3-NF on the calvin cycle, its effects on carboxylation efficiency (A/C_i) (also known as Rubisco carboxylation activity) were determined. When A/C_i was compared between treatment and control *S. natans* plants, 3-NF caused significant decreases, especially at high concentrations, indicating that it could inhibit Rubisco carboxylation activity. Additionally, it is recommended to monitor gas exchange parameters and A/C_i together with fluorescence parameters to determine the effect of organic contaminants on both light and dark reactions (Zhang et al., 2022). Photosystem II (PSII) in thylakoid membranes centered on chlorophyll *a* (Chl a) and chlorophyll *b* (Chl b) absorbs photon energy in the light reaction, which initiates coupled phosphorylation processes and photosynthetic electron transport. The diverse effects of PAHs on treated plants have demonstrated that hydrophobic PAHs can cause conformational changes in thylakoid membranes and accumulate there, disrupting electron transport at both the donor and acceptor sides of PSII. The maximum quantum efficiency (F_v/F_m) of PSII typically determines the process's photon transfer intensity (Han et al., 2022). Previous study showed that certain PAH, such as phenanthrene, reduce the quantum efficiency (Fv/Fm) of electron transport and trapping and damage PSII, which in turn restrict photosynthetic activity (Jin et al., 2017). Decreased F_v/F_m and the efficiency of donation electron to PSI (F_v/F_o) levels obtained from *S.natans* exposed to 3-NF showed that photon transfer performance was negatively impacted, especially at high concentrations. Also, increased F_o/F_m (physiological state of PSII) indicates unbalanced photosynthetic activity. It can be assumed that this is due to the effect of 3-NF on the redox state of its primary electron acceptor, plastoquinone A (Q_A). PAHs can block electron transport in the thylakoid membrane where plastoquinone acts as an electron acceptor or donor (Han et al., 2022). In addition, it has also been reported that the region where the water oxidizing complex (oxygen evolving center, OEC), located in the reaction center of PSII, can also be attacked by PAHs (Lei et al., 2023). Moreover, the performance index (PIABS) determined based on the JIP test is the most sensitive parameter explaining the active reaction center density, light reactions and the efficiency of biochemical reactions (Antunović Dunić et al., 2023). PIABS decreased with 3-NF stress in *S. natans*. This may be due to the decrease in active reaction center density due to toxicity. The decrease in active reaction center density is positively correlated with the increase in energy flux for absorption (ABS/RC) per active reaction centers in *S. natans*, a decrease in energy flux for capture, and electron transport per active reaction center. Therefore, the high energy flux for absorption and its lower utilization resulted in damage to the reaction centers and hence increased heat dissipation (DI_o/RC). The increase in ABS/RC due to 3-NF stress in *S. natans* may be related to the regrouping of light-harvesting complexes of inactive PSII reaction center into the active PSII reaction center, leading to an increase in the conduction of absorbed energy, or to the impairment of electron transfer due to a change in membrane conformation (Ren et al., 2024). Consistent with the results obtained from this study, similar effects of PAHs on the photosynthetic activities of various macrophytes have been previously reported (Minkina et al., 2022).

In plants exposed to organic pollutants such as 3-NF, oxidative stress is induced by the production of reactive oxygen species (ROS) such as hydrogen peroxide, hydroxyl radicals, singlet oxygen and superoxide anion, which have cytotoxic effects in response. Because lipophilic PAH causes induced free radicals to accumulate, it can indirectly alter the structure of the biomembrane. If these radicals cannot be properly scavenged, enhanced lipid peroxidation (TBARS, an indicator product of lipid peroxidation) may follow (Basit et al., 2023; Kösesakal and Seyhan, 2023). Hyperaccumulator plants used for bioremediation must have the capacity to detoxify the effects of ROS by activating antioxidant defense systems to limit ROS-induced damages. Thus, evaluating *S. natans*' antioxidant defense system could provide crucial details regarding the plant's capacity for phytoremediation against 3-NF stress. The antioxidant defense system involves various enzymatic (e.g. superoxide dismutase (SOD), catalase (CAT), gaiacol peroxidase (GPX), glutathione reductase (GR) and glutathione-S-transferase (GST)) and non-enzymatic antioxidants (ascorbic acid, proline, reduced glutathione and carotenoids). These biomolecules also represent molecular bioindicators for oxidative stress mediated by organic pollutants (Tanwir et al., 2021). Nevertheless, ROS also function as signaling molecules with various roles in plant physiology. The crucial enzyme NADPH oxidase (NOX), which is located in the plasma membrane, generates ROS ($O_2^{\bullet-}$), and this NOX-mediated $O_2^{\bullet-}$ signaling initiates antioxidant response in plants under stress conditions (Zhang et al., 2024b). By converting $O_2^{\bullet-}$ into H_2O_2, SOD, the primary antioxidant in plants, initiates the first line of defense against damages resulting from ROS. H_2O_2 is then detoxified by CAT, POX and GPX enzymes or catalyzed by the Asada-Halliwell pathway (AsA-GSH cycle). Up to the 250 μM 3-NF concentration applied in the current study, the H_2O_2 accumulation induced by increasing SOD and NOX activity could be prevented primarily by increasing CAT, POX and GPX enzyme activities at all concentrations (10–25–50-100 μM). In the 10–25-50 μM treatments groups, in addition to these enzymes, the increased activities of APX, GR, MDHAR, DHAR and GST enzymes in the AsA-GSH cycle were also effective in preventing TBARS production by detoxifying H_2O_2. In addition, the highly efficient AsA-GSH regeneration and the preserved tAsA/DHA and GSH redox state seen in these groups support the theory that AsA-GSH regulates plant response mechanisms (Gao et al., 2024) against 3-NF stress in *S. natans*. On the contrary, in the 3-NF100 group, AsA regeneration, which could not be sustained due to the stagnation in MDHAR and DHAR activities, was not effective in preventing H_2O_2 accumulation. As a result, increased antioxidant enzyme activities may be related to the tolerance capacity of *S. natans* to protect the plant from oxidative damage. Consistent with the results obtained by Kavousi et al. (2021) reported increased antioxidant enzyme activity while investigating the phytoremediation potential of *Verbascum thapsus* L. However, in 3-NF applications higher than 250 μM concentration, *S. natans* could not prevent the accumulation of H_2O_2 due to decreased or couldn't be increased enzyme activities, and could not effectively manage tAsA/DHA and GSH/GSSG levels, resulting in high TBARS levels. Similarly, the antioxidant tolerance threshold value for phytoremediation was determined by Levizou et al. (2019) and the possible reason for this situation is associated with the reduced growth rate as a result of excessive accumulation of stress factors in plant parts. *S. natans* was able to grow properly within specific 3-NF concentration ranges, despite increases in 3-NF causing a decrease in plant growth percentage, photosynthetic efficiency, and antioxidant enzyme activities. Furthermore, it was shown that plants showed no obvious symptoms of toxicity stress at concentrations of <250 μM 3-NF. According to these findings, *S. natans* may be cultivated in 3-NF-contaminated waters, making it an

effective strategy for 3-NF phytoremediation.

5. Conclusions

In this study, the phytoremediation capability of *Salvinia natans* for PAH elimination was investigated by the determination and analysis of plant's physiological and biochemical parameters such as 3-NF content, growth, photosynthetic efficiency and antioxidant activity under hydroponic 3-NF stress conditions. According to the findings, *S. natans* is a phytomediator plant that may be categorized as a hyperaccumulator for 3-NF using a variety of methods and is thought to be an effective accumulator. When physiological parameters were evaluated, 3-NF stress had negative impacts on RGR, A, F_v/F_m, and chlorophyll fluorescence at all levels, despite being acceptable at low concentrations. However, because to its active antioxidative defense mechanism, *S. natans* had a high potential for enduring 3-NF toxicity up to an applied dose of 250 μM. AsA regeneration inhibited the accumulation of H_2O_2 and TBARS along with increased SOD, CAT, POX and GPX activities at 10–25-50 μM 3-NF concentrations. Nevertheless, oxidative damage may be avoided even though AsA regeneration could not be achieved in *S. natans* at the dose of 100 μM. >250 μM 3-NF caused oxidative damage in *S. natans*, and this damage could not be alleviated due to inefficient antioxidant enzyme activities. In contrast, *S. natans* has the potential to accumulate 3-NF in the aquatic environment despite the decline in growth and photosynthetic activity and can be used in PAH phytoextraction for polluted aquatic ecosystems without showing signs of oxidative stress up to a certain 3-NF concentration. However, future research is needed on mitigating the effects of 3-NF stress on photosynthesis and physiological parameters in *S. natans*.

CRediT authorship contribution statement

Fatma Nur Alp-Turgut: Writing – review & editing, Writing – original draft, Methodology, Investigation. **Evren Yildiztugay:** Writing – review & editing, Writing – original draft, Methodology, Investigation. **Ceyda Ozfidan-Konakci:** Writing – review & editing, Writing – original draft, Methodology, Investigation. **İsmail Tarhan:** Writing – review & editing, Writing – original draft, Methodology, Investigation. **Melek Öner:** Methodology, Investigation. **Cagri Gulenturk:** Methodology, Investigation.

Declaration of competing interest

The authors declare that they have no known competing financial interests or personal relationships that could have appeared to influence the work reported in this paper.

Data availability statement

The authors declare no competing financial interests.

Acknowledgements

This work was supported by Selcuk University Scientific Research Projects Coordinating Office (Grant Number: 24401168).

Appendix A. Supplementary data

Supplementary data to this article can be found online at https://doi.org/10.1016/j.scitotenv.2024.176335.

References

Adeola, A.O., Forbes, P.B., 2021. Advances in water treatment technologies for removal of polycyclic aromatic hydrocarbons: existing concepts, emerging trends, and future prospects. Water Environ. Res. 93, 343–359.

Akash, S., Sivaprakash, B., Rajamohan, N., Selvankumar, T., 2022. Biotransformation as a tool for remediation of polycyclic aromatic hydrocarbons from polluted environment-review on toxicity and treatment technologies. Environ. Pollut. 120923.

Akinpelumi, V.K., Kumi, K.G., Onyena, A.P., Kabari, S., Ezejiofor, A.N., Frazzoli, C., Ekhator, O.C., Udom, G.J., Orisakwe, O.E., 2023. A comparative study of the impacts of polycyclic aromatic hydrocarbons in water and soils in Nigeria and Ghana: towards a framework for public health protection. Journal of hazardous materials. Advances 100336.

Antunović Dunić, J., Mlinarić, S., Pavlović, I., Lepeduš, H., Salopek Sondi, B., 2023. Comparative analysis of primary photosynthetic reactions assessed by OJIP kinetics in three *Brassica* crops after drought and recovery. Appl. Sci. 13, 3078.

Barbosa Jr., F., Rocha, B.A., Souza, M.C., Bocato, M.Z., Azevedo, L.F., Adeyemi, J.A., Santana, A., Campiglia, A.D., 2023. Polycyclic aromatic hydrocarbons (PAHs): updated aspects of their determination, kinetics in the human body, and toxicity. J. Toxic. Environ. Health, Part B 26, 28–65.

Basit, F., Bhat, J.A., Alyemeni, M.N., Shah, T., Ahmad, P., 2023. Nitric oxide mitigates vanadium toxicity in soybean (*Glycine max* L.) by modulating reactive oxygen species (ROS) and antioxidant system. J. Hazard. Mater. 451, 131085.

Beauchamp, C., Fridovich, I., 1971. Superoxide dismutase: improved assays and an assay applicable to acrylamide gels. Anal. Biochem. 44, 276–287.

Bergmeyer, H.U., 1970. Methoden der enzymatischen Analyse. 2. Verlag Chemie.

Biju, L.M., Kumar, P.S., Kavitha, R., Rajagopal, R., Rangasamy, G., 2023. Application of *Salvinia* sps. In remediation of reactive mixed azo dyes and Cr (VI)-its pathway elucidation. Environ. Res. 216, 114635.

Borah, P., Deka, H., 2024. Polycyclic aromatic hydrocarbon (PAH) accumulation in selected medicinal plants: a mini review. Environ. Sci. Pollut. Res. 1–19.

Bradford, M.M., 1976. A rapid and sensitive method for the quantitation of microgram quantities of protein utilizing the principle of protein-dye binding. Anal. Biochem. 72, 248–254.

Bright, A., Li, F., Movahed, M., Shi, H., Xue, B., 2023. Chronic exposure to low-molecular-weight polycyclic aromatic hydrocarbons promotes lipid accumulation and metabolic inflammation. Biomolecules 13, 196.

Culotta, L., Gianguzza, A., Orecchio, S., 2005. Leaves of *Nerium oleander* L. as bioaccumulators of polycyclic aromatic hydrocarbons (PAH) in the air of Palermo (Italy): extraction and GC-MS analysis, distribution and sources. Polycycl. Aromat. Compd. 25, 327–344.

da Silva Correa, H., Blum, C.T., Galvão, F., Maranho, L.T., 2022. Effects of oil contamination on plant growth and development: a review. Environ. Sci. Pollut. Res. 29, 43501–43515.

Dalton, D.A., Russell, S.A., Hanus, F.J., Pascoe, G.A., Evans, H.J., 1986. Enzymatic-reactions of ascorbate and glutathione that prevent peroxide damage in soybean root-nodules. Proc. Natl. Acad. Sci. U. S. A. 83, 3811–3815.

Dutilleul, C., Driscoll, S., Cornic, G., De Paepe, R., Foyer, C.H., Noctor, G., 2003. Functional mitochondrial complex I is required by tobacco leaves for optimal photosynthetic performance in photorespiratory conditions and during transients. Plant Physiol. 131, 264–275.

Ekperusi, A.O., Nwachukwu, E.O., Sikoki, F.D., 2020. Assessing and modelling the efficacy of *Lemna paucicostata* for the phytoremediation of petroleum hydrocarbons in crude oil-contaminated wetlands. Sci. Rep. 10, 8489.

Foyer, C.H., Halliwell, B., 1976. The presence of glutathione and glutathione reductase in chloroplasts: a proposed role in ascorbic acid metabolism. Planta 133, 21–25.

Fu, X., Walker, B.J., 2023. Dynamic response of photorespiration in fluctuating light environments. J. Exp. Bot. 74, 600–611.

Gao, X., Tan, J., Yi, K., Lin, B., Hao, P., Jin, T., Hua, S., 2024. Elevated ROS levels caused by reductions in GSH and AsA contents lead to grain yield reduction in qingke under continuous cropping. Plants 13, 1003.

Guo, Z., Lv, J., Dong, X., Du, N., Piao, F., 2021. Gamma-aminobutyric acid improves phenanthrene phytotoxicity tolerance in cucumber through the glutathione-dependent system of antioxidant defense. Ecotoxicol. Environ. Saf. 217, 112254.

Han, J., Chang, C.Y.Y., Gu, L., Zhang, Y., Meeker, E.W., Magney, T.S., Walker, A.P., Wen, J., Kira, O., McNaull, S., 2022. The physiological basis for estimating photosynthesis from Chl a fluorescence. New Phytol. 234, 1206–1219.

Hazaimeh, M., Almansoory, A.F., Abd Mutalib, S., Kanaan, B., 2019. Effects of plant density on the bioremediation of soils contaminated with polyaromatic hydrocarbons. Emerging Contaminants 5, 123–127.

He, F., Liu, R., Tian, G., Qi, Y., Wang, T., 2023. Ecotoxicological evaluation of oxidative stress-mediated neurotoxic effects, genetic toxicity, behavioral disorders, and the corresponding mechanisms induced by fluorene-contaminated soil targeted to earthworm (*Eisenia fetida*) brain. Sci. Total Environ. 871, 162014.

Herzog, V., Fahimi, H., 1973. Determination of the activity of peroxidase. Anal. Biochem. 55, e62.

Hossain, M., Hossain, M., Fujita, M., 2006. Induction of pumpkin glutathione S-transferases by different stresses and its possible mechanisms. Biol. Plant. 50, 210–218.

Hou, W.C., Liang, H.J., Wang, C.C., Liu, D.Z., 2004. Detection of glutathione reductase after electrophoresis on native or sodium dodecyl sulfate polyacrylamide gels. Electrophoresis 25, 2926–2931.

Hu, J., Chen, J., Wang, W., Zhu, L., 2023. Mechanism of growth inhibition mediated by disorder of chlorophyll metabolism in rice (*Oryza sativa*) under the stress of three polycyclic aromatic hydrocarbons. Chemosphere 329, 138554.

Huang, Y., Song, Y., Huang, J., Xi, Y., Johnson, D., Liu, H., 2018. Selenium alleviates phytotoxicity of phenanthrene and pyrene in *Alternanthera philoxeroides*. Int. J. Phytoremediation 20, 1438–1445.

Hunt, R., Causton, D.R., Shipley, B., Askew, A.P., 2002. A modern tool for classical plant growth analysis. Ann. Bot. 90, 485–488.

Jia, H., Zhang, G.x., Wu, Y.f., Dai, W.w., Xu, Q.b., Gan, S., Ju, X.y., Feng, Z.z., Li, R.p., Yuan, B., 2023. Evaluation of negative effect of naphthenic acids (NAs) on physiological metabolism and polycyclic aromatic hydrocarbons adsorption of *Phragmites australis*. Chemosphere 318, 137909.

Jiang, M., Zhang, J., 2002. Involvement of plasma-membrane NADPH oxidase in abscisic acid- and water stress-induced antioxidant defense in leaves of maize seedlings. Planta 215, 1022–1030.

Jin, L., Che, X., Zhang, Z., Li, Y., Gao, H., Zhao, S., 2017. The mechanisms by which phenanthrene affects the photosynthetic apparatus of cucumber leaves. Chemosphere 168, 1498–1505.

Kavousi, H.R., Karimi, M.R., Neghab, M.G., 2021. Assessment the copper-induced changes in antioxidant defense mechanisms and copper phytoremediation potential of common mullein (*Verbascum thapsus* L.). Environ. Sci. Pollut. Res. 28, 18070–18080.

Kösesakal, T., Seyhan, M., 2023. Phenanthrene stress response and phytoremediation potential of free-floating fern *Azolla filiculoides* lam. Int. J. Phytoremediation 25, 207–220.

Laemmli, U.K., 1970. Cleavage of structural proteins during the assembly of the head of bacteriophage T4. Nature 227, 680–685.

Lei, Y., Huang, D., Zhou, W., Wang, G., Xiao, R., Xu, W., Huang, H., Li, S., Shen, L., Ren, Y., 2023. Combining phytoremediation with carbon-based materials under carbon neutral background: is it a close step to sustainable restoration? Crit. Rev. Environ. Sci. Technol. 1–22.

Levizou, E., Zanni, A.A., Antoniadis, V., 2019. Varying concentrations of soil chromium (VI) for the exploration of tolerance thresholds and phytoremediation potential of the oregano (*Origanum vulgare*). Environ. Sci. Pollut. Res. 26, 14–23.

Liu, Z.J., Guo, Y.K., Bai, J.G., 2010. Exogenous hydrogen peroxide changes antioxidant enzyme activity and protects ultrastructure in leaves of two *cucumber* ecotypes under osmotic stress. J. Plant Growth Regul. 29, 171–183.

Minkina, T., Fedorenko, A., Nevidomskaya, D., Fedorenko, G., Pol'Shina, T., Sushkova, S., Chaplygin, V., Beschetnikov, V., Dudnikova, T., Chernikova, N., 2022. Uptake of potentially toxic elements and polycyclic aromatic hydrocarbons from the hydromorphic soil and their cellular effects on the *Phragmites australis*. Environ. Pollut. 309, 119727.

Mittler, R., Zilinskas, B.A., 1993. Detection of ascorbate peroxidase-activity in native gels by inhibition of the ascorbate-dependent reduction of nitroblue tetrazolium. Anal. Biochem. 212, 540–546.

Miyake, C., Asada, K., 1992. Thylakoid-bound ascorbate peroxidase in spinach-chloroplasts and photoreduction of its primary oxidation-product monodehydroascorbate radicals in thylakoids. Plant and Cell Physiology 33, 541–553.

Molina, L., Segura, A., 2021. Biochemical and metabolic plant responses toward polycyclic aromatic hydrocarbons and heavy metals present in atmospheric pollution. Plants 10 (11), 2305.

Nakano, Y., Asada, K., 1981. Hydrogen peroxide is scavenged by ascorbate-specific peroxidase in spinach chloroplasts. Plant and Cell Physiology 22, 867–880.

Paradiso, A., Berardino, R., de Pinto, M.C., Sanita di Toppi, L., Storelli, M.M., Tommasi, F., De Gara, L., 2008. Increase in ascorbate-glutathione metabolism as local and precocious systemic responses induced by cadmium in durum wheat plants. Plant Cell Physiol. 49, 362–374.

Rajput, V., Minkina, T., Semenkov, I., Klink, G., Tarigholizadeh, S., Sushkova, S., 2021. Phylogenetic analysis of hyperaccumulator plant species for heavy metals and polycyclic aromatic hydrocarbons. Environ. Geochem. Health 43, 1629–1654.

Rao, K.M., Sresty, T., 2000. Antioxidative parameters in the seedlings of pigeonpea (*Cajanus cajan* (L.) Millspaugh) in response to Zn and Ni stresses. Plant Sci. 157, 113–128.

Ren, H., Lu, Y., Tang, Y., Ren, P., Tang, H., Chen, Q., Kuang, P., Huang, R., Zhu, W., Chen, K., 2024. Photosynthetic responses of *Racomitrium japonicum* L. to strontium stress evaluated through chlorophyll a fluorescence OJIP transient analysis. Plants 13, 591.

Ricci, G., Bello, M.L., Caccuri, A.M., Galiazzo, F., Federici, G., 1984. Detection of glutathione transferase activity on polyacrylamide gels. Anal. Biochem. 143, 226–230.

Sagi, M., Fluhr, R., 2001. Superoxide production by plant homologues of the gp91phox NADPH oxidase. Modulation of activity by calcium and by tobacco mosaic virus infection. Plant Physiol. 126, 1281–1290.

Saha, A., Mukherjee, P., Roy, K., Sen, K., Sanyal, T., 2022. A review on phyto-remediation by aquatic macrophytes: a natural promising tool for sustainable management of ecosystem. International Journal of Experimental Research and Review 27, 9–31.

Seevers, P., Daly, J., Catedral, F., 1971. The role of peroxidase isozymes in resistance to wheat stem rust disease. Plant Physiol. 48, 353–360.

Sharma, J.K., Kumar, N., Singh, N., Santal, A.R., 2023. Phytoremediation technologies and their mechanism for removal of heavy metal from contaminated soil: an approach for a sustainable environment. Front. Plant Sci. 14, 1076876.

Shi, H., Ye, T., Chan, Z., 2013. Exogenous application of hydrogen sulfide donor sodium hydrosulfide enhanced multiple abiotic stress tolerance in bermudagrass (*Cynodon dactylon* (L). Pers.). Plant Physiol. Biochem. 71, 226–234.

Singh, R., Sharma, A., Goswami, P., Pradhananga, D., Aryal, D., Pradhanang, S.M., Kumar, R., 2023. Phytoremediation of Organic Contaminants: An Eco-Friendly Approach-Based Application of Aquatic Macrophytes. Ecology, Functions and Services. Springer, Aquatic Macrophytes, pp. 175–205.

Sitarska, M., Traczewska, T., Hołtra, A., Zamorska Wojdyła, D., Filarowska, W., Hanus Lorenz, B., 2023. Removal of mercury from water by phytoremediation process with *Salvinia natans* L. All. Environmental Science and Pollution Research 30, 85494–85507.

Sivaram, A.K., Subashchandrabose, S.R., Logeshwaran, P., Lockington, R., Naidu, R., Megharaj, M., 2019. Metabolomics reveals defensive mechanisms adapted by maize on exposure to high molecular weight polycyclic aromatic hydrocarbons. Chemosphere 214, 771–780.

Smart, R.E., Bingham, G.E., 1974. Rapid estimates of relative water content. Plant Physiol. 53, 258–260.

Sokol, N.W., Slessarev, E., Marschmann, G.L., Nicolas, A., Blazewicz, S.J., Brodie, E.L., Firestone, M.K., Foley, M.M., Hestrin, R., Hungate, B.A., 2022. Life and death in the soil microbiome: how ecological processes influence biogeochemistry. Nat. Rev. Microbiol. 20, 415–430.

Song, X., Li, C., Chen, W., 2022. Phytoremediation potential of Bermuda grass (*Cynodon dactylon* (L.) pers.) in soils co-contaminated with polycyclic aromatic hydrocarbons and cadmium. Ecotoxicol. Environ. Saf. 234, 113389.

Spinedi, N., Storb, R., Aranda, E., Romani, F., Svriz, M., Varela, S.A., Moreno, J.E., Fracchia, S., Cabrera, J., Batista García, R.A., 2021. ROS-scavenging enzymes as an antioxidant response to high concentration of anthracene in the liverwort *Marchantia polymorpha* L. Plants 10, 1478.

Srivastava, N., 2023. Removal of heavy metal using aquatic macrophytes *Salvinia*. Biochemical & Cellular Archives 23.

Sushkova, S., Minkina, T., Tarigholizadeh, S., Rajput, V., Fedorenko, A., Antonenko, E., Dudnikova, T., Chernikova, N., Yadav, B.K., Batukaev, A., 2021. Soil PAHs contamination effect on the cellular and subcellular organelle changes of *Phragmites australis* Cav. Environ. Geochem. Health 43, 2407–2421.

Tanwir, K., Javed, M.T., Shahid, M., Akram, M.S., Ali, Q., 2021. Antioxidant defense systems in bioremediation of organic pollutants. *Handbook of Bioremediation*. Elsevier 505–521.

Woodbury, W., Spencer, A., Stahmann, M., 1971. An improved procedure using ferricyanide for detecting catalase isozymes. Anal. Biochem. 44, 301–305.

Zazouli, M.A., Asghari, S., Tarrahi, R., Lisar, S.Y.S., Babanezhad, E., Dashtban, N., 2023. The potential of common duckweed (*Lemna minor*) in phytoremediation of phenanthrene and pyrene. Environmental Engineering Research 28.

Zhang, Q., Ficklin, D.L., Manzoni, S., Wang, L., Way, D., Phillips, R.P., Novick, K.A., 2019. Response of ecosystem intrinsic water use efficiency and gross primary productivity to rising vapor pressure deficit. Environ. Res. Lett. 14, 074023.

Zhang, X., Liu, N., Lu, H., Zhu, L., 2022. Molecular mechanism of organic pollutant-induced reduction of carbon fixation and biomass yield in *Oryza sativa* L. Environ. Sci. Technol. 56, 4162–4172.

Zhang, X., Chen, J., Wang, W., Zhu, L., 2024a. Photosynthetic mechanisms of carbon fixation reduction in rice by cadmium and polycyclic aromatic hydrocarbons. Environ. Pollut. 344, 123436.

Zhang, Y., Li, J., Yu, S., Li, W., Dou, Y., Zhang, C., 2024b. Adenosine triphosphate alleviates high temperature-enhanced glyphosate toxicity in maize seedlings. Plant Physiol. Biochem. 210, 108550.

Zhao, C., Xu, J., Shang, D., Zhang, Y., Zhang, J., Xie, H., Kong, Q., Wang, Q., 2021. Application of constructed wetlands in the PAH remediation of surface water: a review. Sci. Total Environ. 780, 146605.